

# Effect of Major Ions on Induction Time of Struvite Precipitation

Işık Kabdaşlı,<sup>a,\*</sup> Simon A. Parsons,<sup>b</sup> and Olcay Tünay<sup>a</sup>

<sup>a</sup>*Istanbul Technical University, Civil Engineering Faculty, Environmental Engineering Department, Ayazağa Kampüsü, 34469, Maslak, Istanbul, Turkey*

<sup>b</sup>*School of Water Sciences, Cranfield University, Cranfield, MK43 0AL, UK*

RECEIVED MARCH 4, 2005; REVISED NOVEMBER 30, 2005; ACCEPTED DECEMBER 16, 2005

*Keywords*  
absorbance monitoring  
impurities  
induction time  
struvite crystal shape  
struvite precipitation  
supersaturation

Struvite precipitation from wastewaters has gained importance as a means of nitrogen and phosphorus treatment and recovery. While the aspects of process modeling and application have been widely studied, little attention was paid to process kinetics. This study attempted to evaluate the induction time of struvite precipitation for low ammonia concentrations and in the presence of ions commonly found in natural waters. Determination of induction time was based on absorbance measurements while conductivity and pH of the solutions were also monitored during the process. Results of the experimental study indicate that the presence of foreign ions is important in determining the induction time along with the degree of supersaturation. The presence of over  $50 \times 10^{-3} \text{ mol dm}^{-3}$  sodium ions retarded induction time significantly. Calcium ions at  $2.5 \times 10^{-4} \text{ mol dm}^{-3}$  concentration caused no marked change in the induction time. While carbonate ions had a slight effect, sulfate ions increased the induction time. Crystal morphology was also observed to be affected by supersaturation and the presence of foreign ions.

## INTRODUCTION

Struvite precipitation has been long studied for a variety of purposes, from biochemistry to waste treatment. Recently, struvite precipitation has been in the focus of studies concerning nutrient recovery from domestic and industrial wastewaters.<sup>1,2</sup> A wide array of wastewaters containing nitrogen or phosphorous has been the subject of struvite precipitation as a means of treatment and recovery. Fertilizer industries, slaughterhouse wastes, tanneries, leachate as well as domestic wastewater sludge supernatants and human urine are among the areas for

which struvite precipitation performance has been investigated in detail.<sup>2–11</sup> Theoretical studies searching for the actual values of thermodynamic constants as well as evaluation of reaction conditions influencing the system performance have been carried out.<sup>12–14</sup> While a substantial number of studies have been conducted for the thermodynamic aspects of the system, *i.e.*, equilibrium modeling, relatively little work has been devoted to kinetics of struvite precipitation.

The kinetics of the system, on the other hand, seems to be rather complex and affected by several parameters. Crystallization kinetics can be evaluated as a two-step

\* Author to whom correspondence should be addressed. (E-mail: [ikabdasli@ins.itu.edu.tr](mailto:ikabdasli@ins.itu.edu.tr))

process: nucleation and growth. Nucleation is the controlling process for induction time. Induction time is defined as the duration between the achievement of supersaturation and appearance of crystals. The appearance of crystals may not necessarily be determined visually. Several different measures have been used for the determination of induction time. Conductivity measurement is a common application where the crystallization process does not change the solution characteristics other than the removal of precipitating ions. Observation of light scintillations,<sup>15</sup> monitoring pH,<sup>16</sup> and absorbance measurements<sup>17</sup> are the other methods employed. Gunn and Murthy<sup>15</sup> studied the concentration dependence of induction time of struvite by light scintillations and found the relation:

$$\Delta t_i = C_i \left[ \left\{ (c(\text{Mg}^{2+})/\text{mol dm}^{-3})(c(\text{NH}_4^+)/\text{mol dm}^{-3}) \right. \right. \\ \left. \left. (c(\text{PO}_4^{3-})/\text{mol dm}^{-3}) \right\}^{1/3} \right]^2 \quad (1)$$

where  $\Delta t_i$  is induction time and  $C_i$  is a constant. They obtained saturated solution by mixing ammonium hydrogen phosphate, magnesium sulfate and ammonium hydroxide solutions. Ohlinger *et al.*<sup>18</sup> used the light scintillation method to determine the induction time of struvite precipitation. Magnesium sulfate and ammonium dihydrogen phosphate solutions were used for precipitation. A linear relation between  $[\log S_a]^{-2}$  and the logarithm of  $t$  was found.  $S_a$  is defined in Eq. (2), where  $a$  indicates ion activities and  $K_{\text{so}}$  is the solubility product.

$$S_a = \left( \frac{[a(\text{Mg}^{2+}) a(\text{NH}_4^+) a(\text{PO}_4^{3-})]_{\text{initial}}}{K_{\text{so, struvite}}} \right)^{1/3} \quad (2)$$

Induction time was found to be influenced by  $S_a$  and, to a lesser degree, by the mixing energy. Abbona *et al.*<sup>13</sup> experimentally studied newberyite and struvite precipitation using ammonium dihydrogen phosphate, ammonia and magnesium sulfate solutions. They concluded that struvite does not nucleate in less than 200 hours for a supersaturation ratio ( $\beta$ ) value lower than 1.3. In their study,  $\beta$  was obtained using Eq. (3).

$$\beta_s = \frac{a(\text{Mg}^{2+}) a(\text{NH}_3) a(\text{HPO}_4^{2-})}{K_{\text{so, struvite}}} \quad (3)$$

Bouropoulos and Koutsoukos<sup>16</sup> determined the induction time of struvite precipitation using ammonium dihydrogen phosphate and magnesium chloride solutions and employing the pH change as an indicator in supersaturation conditions. A wide range of induction times between 6–125 minutes was obtained for the supersaturation ratio of  $\Omega = 3.33$  to 1.13. In this study,  $\Omega$  was obtained using Eq. (4).

$$\Omega = \frac{a(\text{Mg}^{2+}) a(\text{NH}_4^+) a(\text{PO}_4^{3-})}{K_{\text{so, struvite}}} \quad (4)$$

Growth kinetics was found as a second-order dependence on solution supersaturation, implying a surface controlled mechanism. The charge of the precipitated crystals was found to be dependent on magnesium concentration. Isoelectric point was found at  $\text{pMg} = 1.75$ , above which the electrokinetic charge of the particle was negative. At higher magnesium concentrations, a charge reversal occurred and the particles acquired positive charge. Koutsoukos *et al.*<sup>19</sup> studied the effect of foreign ions on struvite precipitation at pH 8.5 and at constant supersaturation. They found that calcium ions retarded the rate of precipitation while malonic acid had no significant effect on the rate of precipitation. Nelson *et al.*<sup>20</sup> studied struvite precipitation kinetics on anaerobic swine lagoon effluent and reported that struvite constituents reached the steady state 35, 45 and 60 minutes after pH adjustment to 9.0, 8.7 and 8.4, respectively. They found that the precipitation rate obeyed first-order kinetics and the rate constant was increasing with increasing pH. The value of the constant was found to be  $3.7 \text{ h}^{-1}$  at pH 8.4. A lag phase of approximately 20 min was observed in struvite formation. Ohlinger *et al.*<sup>21</sup> found that struvite precipitation of a sludge lagoon supernatant in a fluidized bed reactor was a pseudo-first order process with the rate constant  $4.2 \text{ h}^{-1}$  at pH 8.3. Kofina and Koutsoukos<sup>22</sup> found that the morphology of solids was affected by the solution pH. The crystals had needle-like shape at pH 8.5 while orthorhombic crystals formed at pH 9.0. Ivacic *et al.*<sup>23</sup> constructed precipitation diagrams and obtained dissolution kinetics of different struvite morphologies. They found that the sorption of integrating ions was the rate determining mechanism.

The above studies indicate the importance of crystallization kinetics and particularly the role of induction time, which may become the limiting step for struvite precipitation. The pH, mixing energy, supersaturation and the presence of foreign ions are the important factors affecting induction time. The effect of some foreign ions has been claimed to proceed through adsorption onto the surface of crystals and inhibition and/or retardation of the crystal growth.

This study aims to investigate the effect of foreign ions on the induction period of struvite precipitation. Precipitation was set up so as to simulate the actual process. Precipitation pH values were selected to reflect the pH range of struvite precipitation while providing meaningful levels of supersaturation. A low initial ammonia concentration was used to differentiate and compare the system responses to different compositions. Foreign ions used in our study were the common constituents of natural waters as well as wastewaters.

## EXPERIMENTAL

*Materials and Methods*

All experiments were conducted in a cylindrical glass reactor (height 14 cm, diameter 20 cm, effective volume 1500 mL). The system was set up in a temperature controlled room ( $23 \pm 0.1$  °C). Deionized water (conductivity  $0.055 \mu\text{S cm}^{-1}$ ) was provided from a Sartorius Arium 611 model. It was boiled to purge  $\text{CO}_2$  and obtain  $\text{CO}_2$ -free water immediately after being produced and was stored in an airtight bottle for one day before use.  $\text{MgCl}_2 \cdot 6\text{H}_2\text{O}$ ,  $\text{MgO}$  and  $\text{NH}_4\text{H}_2\text{PO}_4$  were used for preparation of stock solutions.  $\text{MgO}$  was dissolved using 1+1 HCl to make up its stock solution when slightly higher chloride concentrations were needed (Runs II and IV). These stock solutions were subjected to vacuum filtration using Millipore membrane filters with a pore size of  $0.22 \mu\text{m}$ . Standardizations of magnesium, phosphate and ammonia stock solutions were done by the EDTA Titrimetric Method, Molybdate/Stannous Chloride Method and Ammonia Titrimetric Method, respectively.<sup>24</sup> Magnesium and ammonia dihydrogen phosphate stock solutions were separately diluted to a final concentration of  $2.45 \times 10^{-3} \text{ mol dm}^{-3}$  after mixing. Initial ammonia concentration was selected in such a way as to represent a typical ammonia concentration of domestic wastewater while providing a reasonable supersaturation at pH 8.5 and 9.0. It also had a magnesium concentration of  $\text{pC} = 2.61$ , which ensures the presence of negatively charged particles of struvite, thus providing an adequate background for the evaluation of electrostatic effects exerted by cations in precipitating solutions.<sup>16</sup> The pH was adjusted in equal volumes (750 mL) of diluted solutions prior to their combination. NaOH solution was used for pH ad-

justments. Additions of calcium, sulfate, carbonate and chloride were made using  $\text{CaCl}_2 \cdot 2\text{H}_2\text{O}$ ,  $\text{Na}_2\text{SO}_4$ ,  $\text{NaHCO}_3$  and NaCl in solid forms, respectively. All chemicals were added into magnesium solutions except for  $\text{NaHCO}_3$ .  $\text{NaHCO}_3$  was added into the ammonia solution to obtain the corresponding pH values. After chemicals addition, the diluted solutions were re-filtered through membrane filters. Diluted solutions were combined and simultaneously rapidly mixed at 500 rpm for 5 seconds, and then the mixing speed was kept constant at 300 rpm in all experiments. A Heidolph MR 3001 model (625 W and 10–1250 rpm) magnetic stirrer was used for stirring. Absorbance was measured on a UV-visible spectrophotometer (Perkin Elmer Lambda 25) at 350 nm light wavelength according to Barrett and Parsons.<sup>25</sup> Absorbance readings were converted to optical density using the 1-cm light path since this may provide a physically more accurate expression where absorbance measurements are made in the presence of particulate matter. Samples were withdrawn using a cut-tip automatic pipette. The pH and conductivity measurement were made with Orion 920 model pHmeter and WTW InoLab Cond Level 2 model conductivity meters, respectively. Absorbance, pH and conductivity measurements were commenced immediately after combination and continued throughout the mixing of solutions for 80 minutes at 1 minute intervals. After precipitation experiments, solutions together with the solid phase were kept for 10 days to ensure equilibrium conditions and were then filtered through membrane filters for measurements. Solid phase micro pictures were taken by Bright Field Microscopy using an Olympus BX 50 camera. All chemicals used were of analytical grade (Merck®). Magnesium, phosphate, ammonia, sulfate and chloride were determined by the EDTA

TABLE I. System Definitions

RUN	Initial pH	Na <sup>+</sup>	Cl <sup>-</sup>	SO <sub>4</sub> <sup>2-</sup>		CO <sub>3</sub> <sup>2-</sup>	Ca <sup>2+</sup>	Ω	Induction time
				10 <sup>3</sup> x mol dm <sup>-3</sup>					
I	8.438	4.8	5.02	–	–	–	–	5.00	7' 51''
II	8.523	6.6	5.16	–	–	–	–	5.76	8' 22''
III	8.555	5.2	5.02	–	–	–	–	6.27	2' 44''
IV	8.551	55.4	55	–	–	–	–	3.89	22'
A	8.489	155.5	155	–	–	–	–	2.35	N.O.
V	8.958	5.8	5.02	–	–	–	–	12.49	50''
VI	8.974	7.1	5.16	–	–	–	–	12.53	1' 26''
VII	9.165	57.4	55	–	–	–	–	10.23	1' 48''
VIII	8.997	157	155	–	–	–	–	5.64	42'
IX	9.196	56	5.02	25	–	–	–	9.37	4' 25''
B	8.996	155.6	5.02	75	–	–	–	4.97	N.O.
X	9.228	156	5.02	75	–	–	–	6.69	46'
XI	9.185	56.4	30.02	12.5	–	–	–	9.82	1' 59''
XII	8.521	4.5	5.02	–	2	–	–	5.93	3' 23''
XIII	9.025	6.0	5.02	–	5	–	–	13.64	1' 40''
XIV	8.547	5.13	5.52	–	–	–	0.25	6.10	3' 30''
XV	8.565	5.14	6.02	–	–	–	0.5	6.25	57''

N.O.: not observed

Titrimetric Method, Molybdate/Stannous Chloride Method, Ammonia Titrimetric Method, Gravimetric Method with Residue Drying, Mercuric Nitrate Method, respectively. All analyses were performed as defined in Standard Methods.<sup>24</sup>

## RESULTS AND DISCUSSION

### Determination of Induction Time

Experimental conditions are defined in Table I. Conductivity changes are given in Figures 1 to 3. Only the experiments with the lowest foreign ion concentration are shown in Figure 1. Experimental results are shown in Figures 2 and 3 for pH 8.5 and pH 9 experiments, respectively. Conductivities were either slightly reduced or remained practically constant during and at the beginning of induction time. Variation of conductivity between the induction time and the end of the experiment was mostly in the form of a decline, though in some cases, particularly for high ionic strengths, it remained virtually constant (*e.g.*, Run IV (6.43 mS cm<sup>-1</sup>), Run VIII (16.39 mS cm<sup>-1</sup>) and Run X (13.63 mS cm<sup>-1</sup>)). The cases of constant conductivity were associated with a slight change in pH (Run VIII and X exhibited pH reductions of 0.034 and 0.056 units, respectively). However, there are cases where significant pH changes occurred at constant or slightly changing conductivities. Examples of these are: Run II (25 μS cm<sup>-1</sup> conductivity change *versus* 0.367 unit pH change) Run IV (10 μS cm<sup>-1</sup> conductivity change *versus* 0.246 unit pH change). Conductivity monitoring did not prove to be an adequate means of induction time determination since it is not a system with a straightforward conductivity reduction as the precipitating ions leave the solution. Struvite precipitation gives rise to the release of hydrogen ions, which have high molar conductivity and also affect the composition of complex species.

pH variations during the experiments are given for pH 8.5 and pH 9 in Figures 4 and 5, respectively. The pH variation from the start of the experiment to the induction time ranged widely in our cases. In Run VIII, pH re-

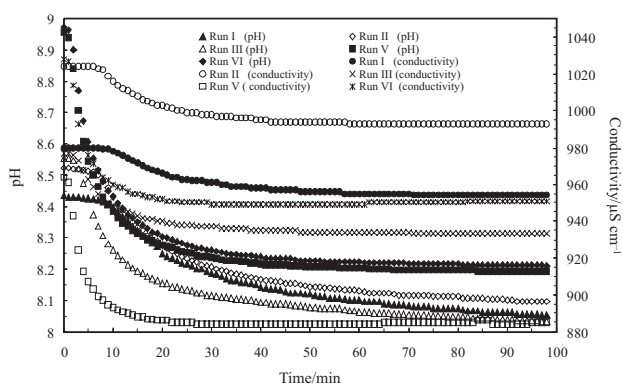


Figure 1. pH and conductivity changes during the experiments with a minimum of foreign ions.

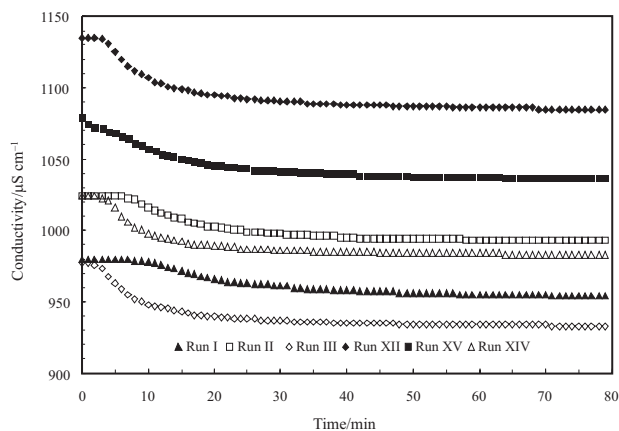


Figure 2. Conductivity changes for pH 8.5 experiments.

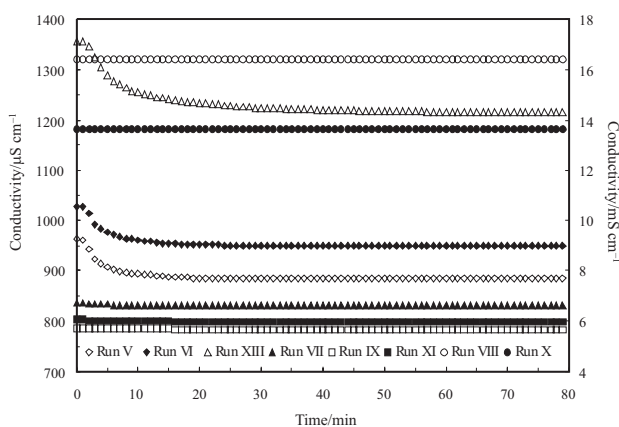


Figure 3. Conductivity changes for pH 9.0 experiments (Runs V, VI, and XIII in μS cm<sup>-1</sup> units; Runs VII, VIII, IX, and X in mS cm<sup>-1</sup> units).

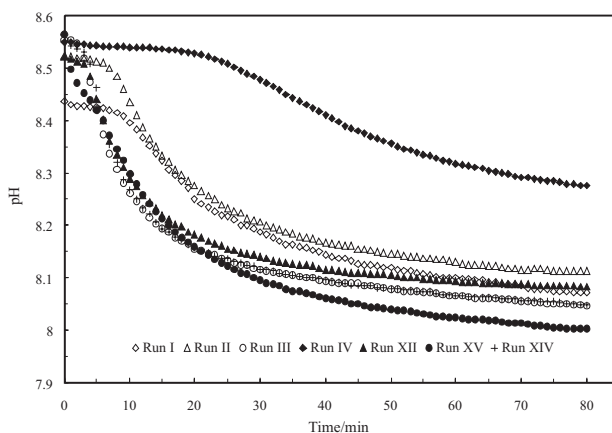


Figure 4. pH changes for pH 8.5 experiments.

mained unchanged until the induction period. The pH change in Runs IX, XI and XII varied between 0.008 and 0.012. However, there were pH variations as high as 0.073 (Runs VI, II and XIV). As noted above, the complexity of the system prevents assessment of the induction

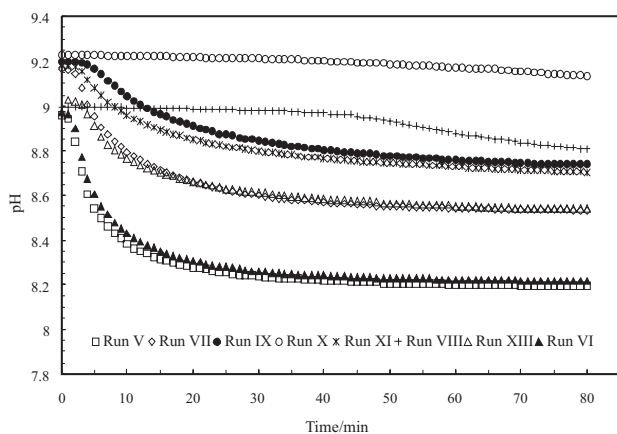


Figure 5. pH changes for pH 9.0 experiments.

time by chemical means in a straightforward way. The system is basically a complex mixture of a weak acid and base. Precipitation reaction does not only affect the system composition through abstraction of ions and release of hydrogen ion but also modifies the buffer capacity of the system and ionic strength of the solution. While the buffer capacity change has a strong effect on the change of pH, ionic strength may exert a significant effect on the solubility. The change in ionic strength through precipitation, however, may be quite low for some cases, *e.g.*, high ionic strength due to foreign ions. The use of pH increment of 0.005 units as an indication of induction time for struvite precipitation by Bouropoulos and Koutsoukos<sup>16</sup> may be taken to imply initiation of the precipitation reaction rather than the operational definition of induction time.

Monitoring of the optical density proved to be a reliable means for determination of the induction time of struvite precipitation in our study. In all the experiments, the first significant increase in optical density that was recognized as the end of the induction period was immediately followed by turbidity observable by the naked eye. Changes in optical density following the induction time were gradual and reached stable values after 15–80 minutes in all systems. Optical density recordings for the experiments are depicted in Figures 6, 7 and 8. Figure 6 presents the results for a minimum of foreign ions, *i.e.*, originating from the addition of precipitation reagents and pH adjustment. Figures 7 and 8 show the results of struvite precipitation conducted at pH 8.5 and 9, respectively.

#### Effect of Foreign Ions on Induction Time

Experimental results are outlined in Table I with the induction times based on optical density measurements.  $\Omega$  values tabulated in the table were obtained using Eq. (3). Ion activities in this equation were calculated using a model proposed by Kabdašli *et al.*,<sup>17</sup> which is given in Appendix A.

The first two experiments described in Table I (Runs I and II) were designed to evaluate the effect of sodium concentration on the induction time. In these experiments, chloride concentrations were kept at the same level but

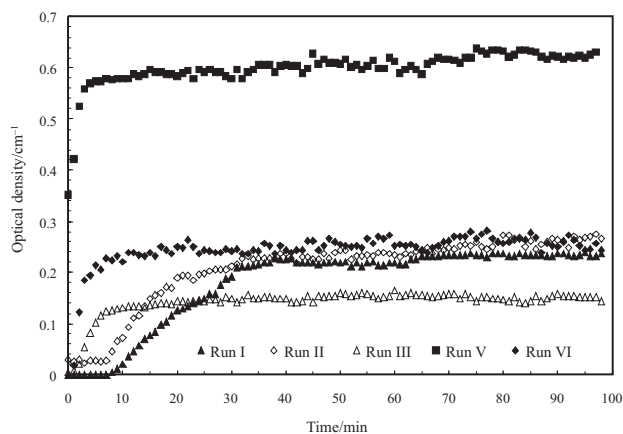


Figure 6. Optical density changes during the experiments with a minimum of foreign ions.

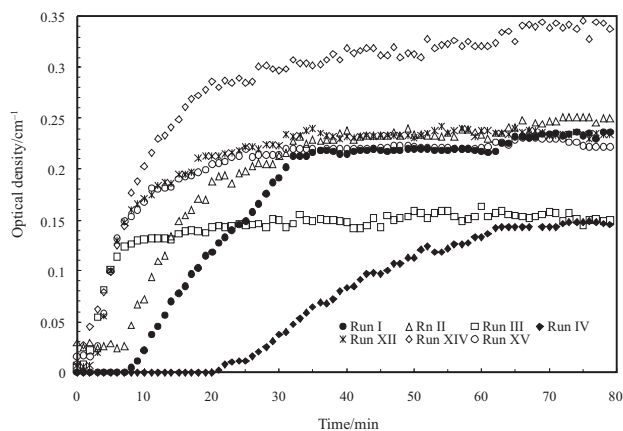


Figure 7. Optical density changes for pH 8.5 experiments.

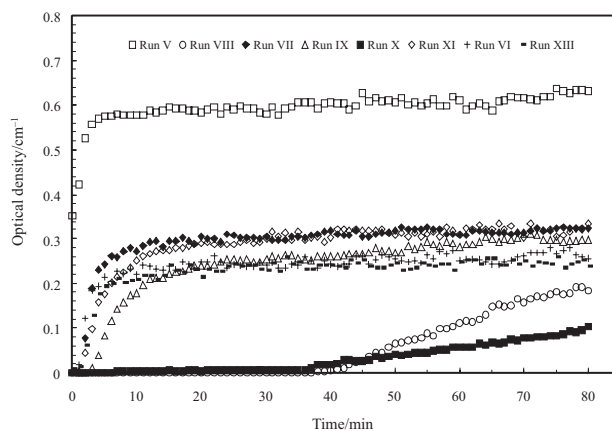


Figure 8. Optical density changes for pH 9 experiments.



sodium concentration was changed by about 35%. The initial pH was tried to be kept constant. However, this required pH adjustment following the addition of solutions and this was avoided for the systems having short induction time. The increase in sodium concentration in Run II caused a slight increase in the induction time despite the increase in supersaturation, which was expected to shorten the induction time. This may be attributed to accumulation of positively charged sodium ions around negatively charged molecule groups of struvite. If the pH of this experiment were at the same level with that of Run I, this effect could be more pronounced, because as indicated by Run III a further but slight increase in the pH increased the supersaturation and resulted in a significant reduction of induction time. In Run IV, the level of sodium ions was increased more than tenfold by adding  $50 \times 10^{-3} \text{ mol dm}^{-3}$  sodium, while the pH level of Runs II and III was maintained. The results indicate a reduction in the magnitude of induction time. This reduction was due to the combined effect of decreasing supersaturation and increasing sodium concentration. Run A was deliberately conducted at a slightly lower pH and at a much higher sodium concentration while the level of supersaturation was close to that of Run IV. The result of this experiment indicates a rather stable supersaturated system where crystallization was hindered.

Higher degrees of supersaturation were provided by the elevation of pH to 9.0, which is the most commonly applied pH value in the struvite precipitation practice. Runs V and VI were replications of Runs I and II at pH 9.0 and their results exhibited a strong parallelism in terms of the level of supersaturation and the difference between sodium concentrations, except for the magnitude of induction time, which was considerably shorter at pH 9.0 due to the increasing driving force. Increase in the induction time by addition of  $50 \times 10^{-3} \text{ mol dm}^{-3}$  sodium, however, was much lower with respect to lower pH, as indicated by the results of Run VII. But, this difference would have been relatively greater if the supersaturation of Run VII could have been kept at the level of Runs V and VI. However, the result of Run VIII, although it had lower supersaturation than Runs V and VI, strengthened the conclusion about the role of sodium ions in induction time. Realization of precipitation, as compared to Run A, was due to a significant difference in supersaturation between Runs A and VII. The required induction time at this sodium level seemed to be at the limit of practical applicability. This sodium concentration can be encountered in some wastewaters, such as of leather tanning or landfill leachate, which are the potential areas for the application of struvite precipitation.

Further experiments were conducted by replacing the chloride with sulfate. Comparison with Runs VII and IX, where both pH and sodium concentration were close to

one another and supersaturations were comparable, showed that the existence of sulfate increased the induction time. This effect was confirmed by the result of Run XI where the induction time was reduced close to that of the sodium chloride matrix as the sulfate level decreased. Increasing the sodium level along with sulfate resulted in a stable solution (Run B) in spite of higher supersaturation (*cf.* Run A). This effect could be compensated by increasing the pH to 9.228 and supersaturation to 6.69 (a comparable value with that of Run VIII) in Run X while the induction time was still too high.

The effect of carbonate ions on struvite precipitation was studied by Run XII. Comparison of the result of Run XII with Run I may show that the reduction in induction time can be attributed to higher supersaturation and reduced sodium concentration. On the other hand, Runs XII and III had the same level of supersaturation and induction times were of the same magnitude for both cases. Run XIII was aimed to observe the effect of carbonate ions at pH 9.0 and a high supersaturation ratio. Comparison of the results of Runs V and XIII where the precipitation conditions were similar, justified the result of the experiment conducted at pH 8.5, though the carbonate concentration increased to  $5 \times 10^{-3} \text{ mol dm}^{-3}$  at pH 9.0, yielding a high supersaturation ratio. These results indicate that the effect of carbonate could be assumed to be marginal.

Runs XIV and XV were conducted to show the effect of the presence of calcium ions. Reaction conditions of Runs XV and III were quite similar, providing a suitable case for comparison. Calcium, being a cation with two positive charges, was expected to decelerate induction time. This effect was demonstrated by Koutsoukos *et al.*<sup>19</sup> for very low calcium concentrations of 0.5 and 1  $\text{mg L}^{-1}$ . But this effect seemed to be very slight when Runs III and XIV were compared. In Run XV, the picture was different and increasing the calcium concentration reduced the induction time while supersaturation ratios of Runs XV and III were almost the same.

### *Crystal Morphology*

The micro-pictures of crystals obtained in the experiments are shown in Figure 9. The first three pictures (Runs II, III and IV) showed similar crystal shapes and dimensions. At pH 9 and at low and medium sodium concentrations (Runs V and VII), the crystals were just a little larger than those of Runs II and IV. At a high sodium concentration, the crystal width became longer (Run VIII). Run IX exhibited again needle-like crystals. The crystals of Run X were slightly larger than those of Run IX. Crystal shapes and dimensions of Runs XII and XIII were similar. The crystals of Runs XIV and XV, whose solution contains calcium, were larger than other crystals.

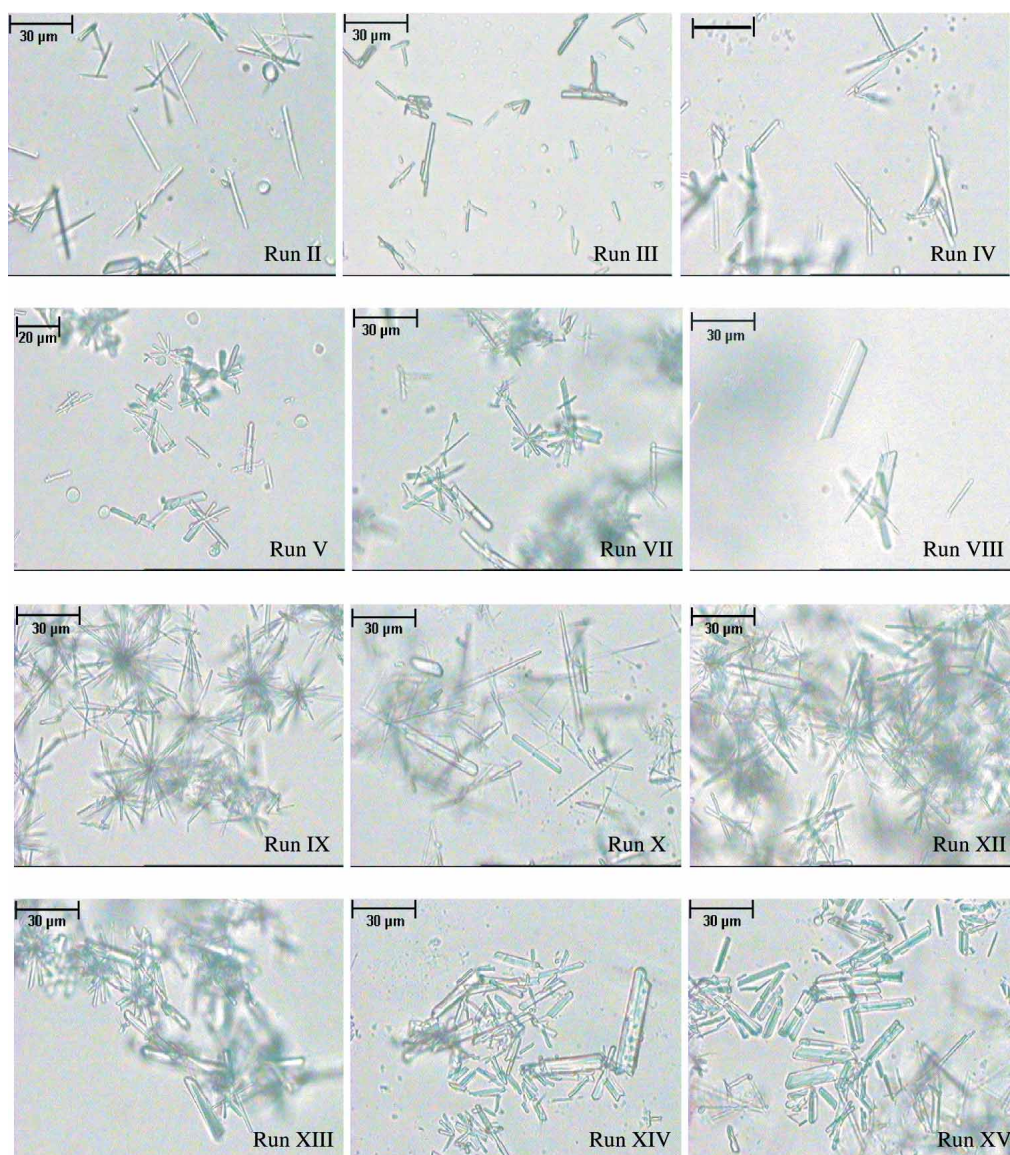


Figure 9. Morphology of struvite crystals obtained in experiments (magnification:  $\times 400$ ).

## CONCLUSIONS

In this paper, the induction time of struvite precipitation was experimentally studied for a low ammonia concentration. Effect of common ions on induction time was determined for the concentration range encountered in surface waters. Optical density monitoring proved to be a sensitive method of induction time determination. Induction time varied in a wide range, depending on the solution composition. Although supersaturation had a considerable effect on induction time, the existence of some ions seemed dominant and became the determining factor for the length of induction time. The existence of sodium ions over  $50 \times 10^{-3} \text{ mol dm}^{-3}$  extended the induction time. The effect of calcium was found to be more complex but not drastic at a low concentration of  $2.5 \times 10^{-4} \text{ mol dm}^{-3}$ . Sulfate ions caused increased in-

duction times. The presence of carbonate-bicarbonate ions had a slight effect on the induction time. Crystal morphology and dimensions were affected by supersaturation and the presence of foreign ions.

## Appendix A

A theoretical model<sup>17</sup> has been developed in order to calculate the activities of species being formed in the  $\text{MgCl}_2\text{-NH}_4\text{H}_2\text{PO}_4\text{-NaOH-H}_2\text{O}$  system. This model takes into account the chemical equilibrium equations given in Table AI, except for the struvite formation reaction, which was used to calculate  $\Omega$ . The following mass balance equations for all species and the electroneutrality condition together with all chemical equilibrium equations (A1–A9) were used in the model.

TABLE A1. The species taken into account by the theoretical model

	log <i>K</i>
(A1) $H^+ + PO_4^{3-} \leftrightarrow HPO_4^{2-}$	12.37 <sup>(a)</sup>
(A2) $H^+ + HPO_4^{2-} \leftrightarrow H_2PO_4^-$	7.20 <sup>(a)</sup>
(A3) $H^+ + H_2PO_4^- \leftrightarrow H_3PO_4$	2.15 <sup>(a)</sup>
(A4) $Mg^{2+} + PO_4^{3-} \leftrightarrow MgPO_4^-$	4.80 <sup>(a)</sup>
(A5) $Mg^{2+} + HPO_4^{2-} \leftrightarrow MgHPO_4^0$	2.80 <sup>(a)</sup>
(A6) $Mg^{2+} + H_2PO_4^- \leftrightarrow MgH_2PO_4^+$	0.45 <sup>(a)</sup>
(A7) $Mg^{2+} + OH^- \leftrightarrow MgOH^+$	2.60 <sup>(a)</sup>
(A8) $H^+ + NH_3 \leftrightarrow NH_4^+$	9.24 <sup>(a)</sup>
(A9) $H^+ + OH^- \leftrightarrow H_2O$	14 <sup>(a)</sup>
(A10) $H^+ + HCO_3^- \leftrightarrow H_2CO_3^*$	6.33 <sup>(a)</sup>
(A11) $H^+ + CO_3^{2-} \leftrightarrow HCO_3^-$	10.33 <sup>(a)</sup>
(A12) $NH_4^+ + Mg^{2+} + PO_4^{3-} \leftrightarrow MgNH_4PO_4 \cdot 6H_2O(s)$	13.26 <sup>(b)</sup>

(a) Refs. 26,27.

(b) Ref. 14.

Mass balance for ammonia species (all species are in mol dm<sup>-3</sup> units in the equation);

$$c(N_{\text{tot}}) = c(NH_3) + c(NH_4^+) \quad (\text{A13})$$

Mass balance of magnesium species (all species are in mol dm<sup>-3</sup> units in the equation);

$$c(Mg_{\text{tot}}) = c(Mg^{2+}) + c(MgH_2PO_4^+) + c(MgHPO_4^0) + c(MgPO_4^-) + c(MgOH^+) \quad (\text{A14})$$

Mass balance of phosphate species (all species are in mol dm<sup>-3</sup> units in the equation);

$$c(P_{\text{tot}}) = c(H_3PO_4) + c(H_2PO_4^-) + c(HPO_4^{2-}) + c(PO_4^{3-}) + c(MgH_2PO_4^+) + c(MgHPO_4^0) + c(MgPO_4^-) \quad (\text{A15})$$

Mass balance of sodium (all species are in mol dm<sup>-3</sup> units in the equation);

$$c(Na_{\text{tot}}) = c(Na^+) \quad (\text{A16})$$

Mass balance of chloride (all species are in mol dm<sup>-3</sup> units in the equation);

$$c(Cl_{\text{tot}}) = c(Cl^-) \quad (\text{A17})$$

Electroneutrality condition (all species are in mol dm<sup>-3</sup> units in the equation);

$$c(H^+) + c(NH_4^+) + 2 \times c(Mg^{2+}) + c(MgH_2PO_4^+) + c(MgOH^+) + c(Na^+) = c(OH^-) + c(Cl^-) + c(H_2PO_4^-) + 2 \times c(HPO_4^{2-}) + 3 \times c(PO_4^{3-}) + c(MgPO_4^-) \quad (\text{A18})$$

There are 15 species and Equations A1–A9 and A13–A20 were used for the theoretical solution for the

MgCl<sub>2</sub>-NH<sub>4</sub>H<sub>2</sub>PO<sub>4</sub>-NaOH-H<sub>2</sub>O system. For addition of sulfate, only the SO<sub>4</sub><sup>2-</sup> species, for addition of carbonate the H<sub>2</sub>CO<sub>3</sub><sup>\*</sup>, HCO<sub>3</sub><sup>-</sup> and CO<sub>3</sub><sup>2-</sup> species and for addition of calcium the Ca<sup>2+</sup> species were added to the system. For carbonate addition, equilibrium equations A10 and A11 were used. Equation A18 was modified accordingly for all systems and related mass balance equations were incorporated into the model. Ionic strength was also taken as a variable, defined as:

$$I = 0.5 \times \sum c_i(z_i)^2 \quad (\text{A19})$$

A commercial spreadsheet was used to solve the theoretical model based on iterative calculation for a given pH. All dissociation and stability constants used were chosen for 25 °C and zero corrected ionic strength. Ionic strength correction was made by using the modified form of Debye-Hückel equation proposed by Davies:

$$\log \gamma_z = -Az_{\pm}^2 \left[ \left( \frac{(I / \text{mol dm}^{-3})^{1/2}}{1 + (I / \text{mol dm}^{-3})^{1/2}} \right) - 0.3I / \text{mol dm}^{-3} \right] \quad (\text{A20})$$

where *I* is ionic strength, *z*<sub>±</sub> is the charge of ionic species, *γ*<sub>*z*</sub> is the species activity coefficient and *A* is the Debye-Hückel constant, which is a function of the temperature and dielectric constant of the solution (0.509 at 25 °C).

## REFERENCES

1. J. Doyle and S. A. Parsons, *Water Res.* **36** (2002) 3925–3940.
2. I. Kabdaşlı, T. Ölmez, and O. Tünay, *Water Sci. Tech.* **48** (2003) 215–223.
3. M. W. Zdybiewka and B. Kula, *Water Sci. Technol.* **24** (1991) 229–234.
4. O. Tünay, I. Kabdaşlı, D. Orhon, and S. Kolçak, *Water Sci. Technol.* **36** (1997) 225–228.
5. I. Kabdaşlı, O. Tünay, I. Öztürk, Z. Yılmaz, and O. Arıkan, *Water Sci. Technol.* **41** (2000) 237–240.
6. I. Kabdaşlı, M. Gürel, and O. Tünay, *Environmental Technol.* **21** (2000) 1147–1155.
7. I. Kabdaşlı, O. Tünay, M. Ş. Çetin, and T. Ölmez, *Water Sci. Technol.* **46** (2002) 231–239.
8. G. Zengin, T. Ölmez, S. Dogruel, I. Kabdaşlı, and O. Tünay, *Water Sci. Technol.* **45** (2002) 205–215.
9. I. Kabdaşlı, O. Tünay, and P. Özcan, In: E. Choi and Z. Yun (Eds.), *IWA Sixth Specialty Symposium on Strong Nitrogenous and Agro Wastewater*, Korea, 2003, pp. 971–978.
10. I. Kabdaşlı, O. Tünay, M. B. Tatlı and S. Topcuoglu, *Fresenius Environ. Bull.* 2006 (in press).
11. I. Kabdaşlı, O. Tünay, Ç. İşlek, E. Erdinç, S. Hüskalar, and M. B. Tatlı, *Water Sci. Technol.* 2006 (in press).
12. F. Abbona and R. Boistelle, *J. Crystal Growth* **46** (1979) 339–354.



13. F. Abbona, H. E. L. Madsen, and R. Boistelle, *J. Crystal Growth* **57** (1982) 6–14.
14. K. N. Ohlinger, T. M. Young, and E. D. Schroeder, *Water Res.* **32** (1998) 3607–3614.
15. D. J. Gunn and M. S. Murthy, *Chem. Eng. Sci.* **17** (1972) 1293–1313.
16. N. Bouropoulos and P. G. Koutsoukos, *J. Crystal Growth* **213** (2000) 381–388.
17. I. Kabdašli, D. Nkansah, and S. A. Parsons, *Environmental Technol.* 2005, in press.
18. K. N. Ohlinger, T. M. Young, and E. D. Schroeder, *J. Environmental Eng.* **125** (1999) 730–737.
19. P. G. Koutsoukos, A. N. Kofina, and P. G. Klepetsanis, *WASIC Conference (Workshop on Advance in Sensoring in Industrial Crystallization)*, Istanbul, Turkey, 2003.
20. N. O. Nelson, R. L. Mikkelsen, and D. L. Hesterberg, *Bio-resource Technol.* **89** (2003) 229–236.
21. K. N. Ohlinger, T. M. Young, and E. D. Schroeder, *J. Environmental Eng.* **126** (2000) 361–368.
22. A. N. Kofina and P. G. Koutsoukos, *WASIC Conference (Workshop on Advance in Sensoring in Industrial Crystallization)*, Istanbul, Turkey, 2003.
23. V. B. Ivančić, J. Kontrec, D. Kralj, and L. Brečević, *Croat. Chem. Acta* **75** (2002) 89–106.
24. American Public Health Association, American Water Works Association, Water Environment Federation, *Standard Methods for the Examination of Water and Wastewater*, 20th ed., APHA, Washington DC, 1998.
25. R. A. Barrett and S. A. Parsons, *Water Res.* **32** (1998) 609–612.
26. L. G. Sillen and A. E. Martell, *Stability Constants of Metal-Ion Complexes*. Special Publ. No. 17, The Chemical Society, London, UK, 1964.
27. L. G. Sillen and A. E. Martell, *Stability Constants of Metal-Ion Complexes*. Special Publ. No. 25, The Chemical Society, London, UK, 1971.

---

## SAŽETAK

### Djelovanje glavnih iona na induksijsko vrijeme taloženja struvita

Işık Kabdaşlı, Simon A. Parsons i Olcay Tünay

Taloženje struvita iz otpadnih voda od značajne je važnosti zbog mogućnosti istodobnog uklanjanja dušika i fosfora. Pri tome je u objavljenim istraživanjima pretežiti naglasak na modeliranju procesa i njegovoj primjeni, dok je važnost kinetike djelomično zanemarivana. U ovom je radu izučavano induksijsko vrijeme taloženja struvita iz vodenih otopina koje su sadržavale niske koncentracije amonijaka, te ione koji se uobičajeno nalaze u prirodnim vodama. Induksijsko je vrijeme određivano mjerenjem optičke propusnosti otopina, pri čemu je također kontinuirano mjerena njena provodljivost i pH. Dobiveni rezultati ukazuju na značaj ovisnosti induksijskog vremena kako o prisutnim stranim ionima tako i o stupnju zasićenosti otopine. Utvrđeno je da dodatak natrijevih iona u koncentracijama višim od  $50 \cdot 10^{-3} \text{ mol dm}^{-3}$  znatno produljuje induksijsko vrijeme, dok kalcijevi ioni pri koncentraciji od  $2,5 \cdot 10^{-4} \text{ mol dm}^{-3}$  ne uzrokuju značajne promjene. Učinak karbonatnih iona na induksijsko vrijeme taloženja struvita je malen, dok ga sulfatni ioni produljuju. Također je utvrđeno da morfologija kristala struvita ovisi o prezasićenosti otopine i o prisutnosti stranih iona.